

ANALYSIS AND REDESIGN OF SPOKES ON ROTARY KILN

Adrien Chereau, Fahimeh Shakibapour, Ioakeim Dourlios, Karim A. Moaty and Yang-Che Lin

Department of Mechanical and Manufacturing Engineering, Aalborg University
 Fibigerstraede 16, DK-9220 Aalborg East, Denmark
 Email: achere17, fshaki16, idourl16, kmoaty16, ylin16@student.aau.dk,
 Web page: <http://www.mechman.m-tech.aau.dk/>

Abstract

In asphalt mixing plants, the rotary kiln is a massive machine whose function is to dry and heat a mixture of sand and gravel. The rotation of the kiln is transferred through supporting rings which are fitted to the drum shell by means of spokes. Loads acting on these spokes are both thermal and mechanical. Indeed, the rotary kiln is highly heated by a burner and loaded as well by its self-weight and the raw material passing through it. The spokes are welded onto both the supporting ring and the drum shell. Fatigue can lead after some time of operation to spoke or weld crack. In this article, a load investigation is carried out using analytical and numerical approaches. Stress results are obtained by finite element simulation and numerical model is compared with strain gauge measurements performed on an operating rotary kiln. Then, fatigue analysis is conducted to find the expected lifetime of both the spoke and the welds. Finally, an optimized redesign of the spoke is presented to improve fatigue lifetime.

Keywords: Rotary kiln, Fatigue, Finite Element Analysis, Welded joints, Optimization, Redesign

1. Introduction

Rotary kilns are extensively used for asphalt, cement and in other industries because of their efficient mixing performance and heat transfer capacity [1]. In asphalt production, their function is to provide a first mix and raise raw material, composed of sand and aggregates, to a high temperature. Raw material is fed into the rotary kiln from one end and a burner supplies heat at the other end, as shown in Fig.1.

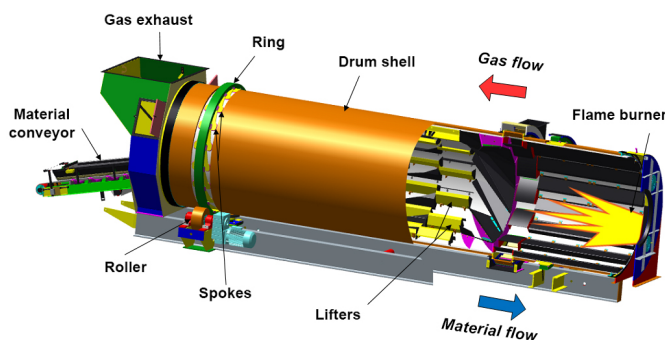


Fig. 1 Elements of rotary kiln studied

The studied rotary kiln employs two ring-roller stations, each with eighteen welded spokes, to transmit torque from rotating rollers to the drum shell. During operation, spokes are cyclically loaded by the self-weight of the structure as well as the raw material passing by. In worst case scenarios both loads combined can reach more than 30 tons. In addition, the temperature of the drum shell at

the burner end can reach around $400^{\circ}C$ creating a large gradient of temperature throughout the rotary kiln. The temperature difference imposes a significant additional load on the spokes.

Fatigue is a main concern here since crack formations are noticed on both spokes and welds. On the cold side of the kiln (i.e. far away from the burner), cracks appear on the spoke (see Fig.2), whereas they initiate on the welds on the hot side (i.e. close to the burner). These failures require maintenance and repairing procedures which are costly as well as time-consuming.

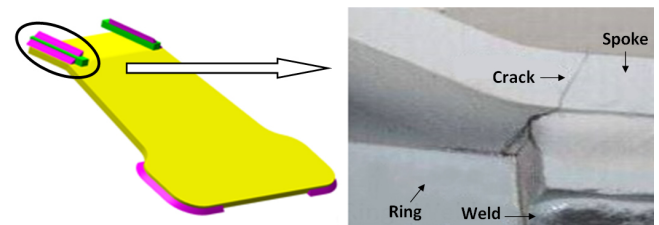


Fig. 2 Spoke and crack propagation on the cold side

This paper focuses on detailed analysis and redesign of the kiln spokes on the cold side. Firstly, a load model is built considering both mechanical and thermal loads. Numerical analysis is then carried out to extract stress results for fatigue analysis. To verify the simulation model, strain gauge measurements are performed on an operating rotary kiln. Finally, an improved lifetime spoke is designed using optimization methods.

2. Load model

To approximate the load acting on the rotary kiln in a steady-state, a static model is taken into consideration. Consequently, dynamic effects as torsion on spokes at start or cascading bed motion are neglected. The loads acting on the 10-meter long kiln can be categorized as the self-weight of the kiln (15 tons), the raw material (16 tons) and the thermal load due to the burner. All components are made of structural steel. The drum is assumed parallel with the ground and other specifications are given in Tab.I.

Reaction force of the rollers F	151 kN
Outer drum shell radius R_1	1235 mm
Inner ring radius R_1'	1320 mm
Outer ring radius R_2	1415 mm
Angle of rollers wrt. vertical axis	37°
Rotating speed of the kiln	8 rpm

Tab. I Specifications of rotary kiln studied

An analytical model is built to study the influence of mechanical load. Besides that, the thermal load is taken into account in the numerical model.

2.1 Mechanical Load

Based on research presented in [2], a two-dimensional (2D) static analysis is performed to obtain bending stress distribution on the ring (spokes are omitted here). In order to model the reality more accurately, the raw material inside the rotary kiln is considered to be unevenly distributed (i.e. bed motion) as shown in Fig.3.

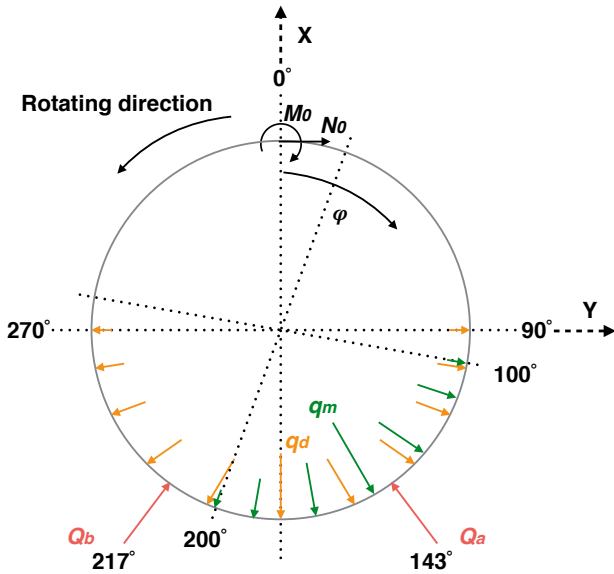


Fig. 3 Two-dimension model with uneven load distribution

The distributed loads q_d and q_m represent the self-weight of kiln and raw material, respectively. Q_a and Q_b are the reaction forces contributed by the two supporting rollers. M_0 is the bending moment and N_0 is the horizontal force acting on the cross section. Both q_d and q_m are assumed to be functions of cosine and can be expressed as Eq.1. The resultant forces of q_d and q_m are denoted as Q_d and Q_m , respectively. The coefficients in Eq.1 are determined by assuming (a) the summation of Q_d and Q_m in X-direction is equal to F and (b) $Q_d = Q_m$ due to the fact that the weight of the kiln and raw material are almost the same.

$$q_d = \frac{0.3412 \cdot F}{R_1} \cdot \cos(\varphi) \quad (1)$$

$$q_m = \frac{0.5188 \cdot F}{R_1} \cdot \cos\left(\frac{9}{5}\varphi - \frac{\pi}{2}\right)$$

In order to find bending stress distribution on the ring, moment must be considered first. The ring can be treated as a curved beam. The bending moment M_b acting on the ring can be found by Eq.2, where M_{q_d} and M_{q_m} are the moment caused by q_d and q_m , respectively and $R_{avg} = (R_1 + R_2)/2$.

$$M_b = M_0 + N_0 R_{avg} (1 - \cos \varphi) + M_{q_d} + M_{q_m} - Q_a R_{avg} \sin\left(\varphi - \frac{5\pi}{6}\right) - Q_b R_{avg} \sin\left(\varphi - \frac{7\pi}{6}\right) \quad (2)$$

By applying Castigliano theorem, M_0 and N_0 can be determined as shown in Eq.3. $\alpha|_{\varphi=0}$ is the rotation angle and $\delta|_{\varphi=0}$ is the horizontal displacement at $\varphi = 0$. Note that since the material is not evenly distributed, they are not exactly zero but have negligible values.

$$\alpha|_{\varphi=0} = \frac{\partial U}{\partial M_0} \Big|_{\varphi=0} = \frac{R_{avg}}{EI} \int_0^\pi 2M_b \cdot \frac{\partial M_b}{\partial M_0} d\varphi = 0$$

$$\delta|_{\varphi=0} = \frac{\partial U}{\partial N_0} \Big|_{\varphi=0} = \frac{R_{avg}}{EI} \int_0^\pi 2M_b \cdot \frac{\partial M_b}{\partial N_0} d\varphi = 0 \quad (3)$$

Finally, the bending stress σ_b on the inner surface of the ring (i.e. on the drum shell) can be found by Eq.4 [2], where A is the area of the ring cross section and $R_n = (R_2 - R_1) / \ln(R_2/R_1)$. The distribution is presented in Fig.4.

$$\sigma_b = \frac{M_b (R_n - R_1)}{AR_1 (R_{avg} - R_n)} \quad (4)$$

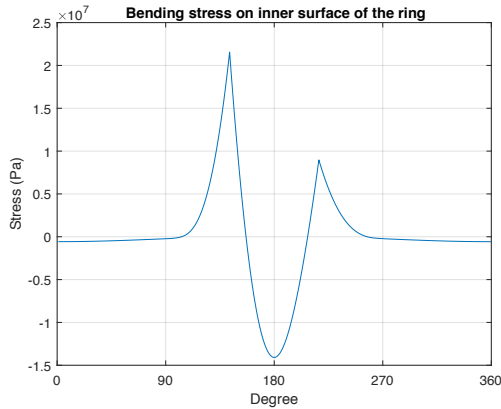


Fig. 4 Bending stress on the inner surface of the ring

Instead of one single ring, the rotary kiln studied in this article has a set of spokes between the drum and the ring. Therefore, this analytical model is not directly used but it provides an understanding of stress distribution on the drum shell. Furthermore, distributed loads q_d and q_m are reutilized in the numerical model.

2.2 Thermal Load

Given the rotary kiln is heated by a burner, components are subjected to thermal expansion which implies thermal stresses, especially on the spokes. This occurs because the shell and the ring do not have the same temperature creating a significant temperature difference on the spoke, even on the cold side. The spokes are welded onto both the shell and the ring and therefore their expansion are restricted at both ends which results in thermal stresses.

In order to obtain thermal stresses on the spokes, analysis is done in the numerical model which is elaborated in section 3.2. However, a general understanding of the basic principles of heat transfer and the coefficients needed for the Finite Element Analysis (FEA) are discussed first. Basically, there are three modes of heat transfer: conduction, convection and radiation which require to define temperature distribution, heat transfer coefficient and emissivity, respectively [3].

Heat transfer coefficient for spokes is found in tables from reference [3]. To obtain temperature field and emissivity of the spokes, an experiment is taken into consideration using an infrared (IR) camera. In an IR thermography application, object's surface emissivity is crucial since it significantly impacts the temperature measurement results. Different methods exist in order to obtain it [4]. The method applied in this case is by using thermometer working parallel to the camera, spoke's

emissivity has been measured to 0,93. Afterwards, the temperature distribution for spokes on the cold side of the rotary kiln is captured and is shown in Fig.5.

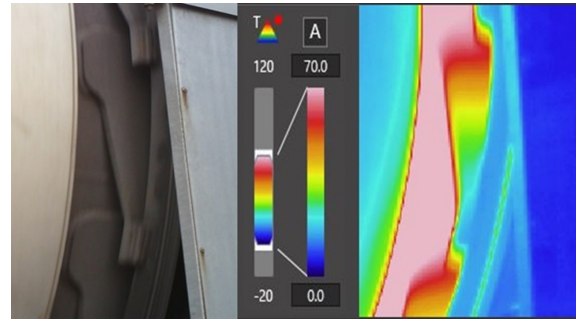


Fig. 5 Temperature distribution for spokes captured by IR camera ($^{\circ}C$)

3. Finite Element Analysis

FEA is considered here because it is hard to predict boundary conditions of the spokes analytically. In addition, it is convenient to extract results for fatigue analysis of the spokes and the welds as well as performing shape optimization. A three-dimensional (3D) model of the rotary kiln is therefore studied using ANSYS Workbench with the actual boundary conditions. Accurate results on local areas can be obtained using submodeling procedure from the rough model.

3.1 Submodeling

The full 3D geometry of the rotary kiln is modeled for different reasons. The first one is because only loads acting on the entire structure are known. The other reason is that no symmetric simplification can be done because of the unevenly distributed load (bed motion) and the position of the kiln with respect to the rollers. As shown in Fig.6 (a), only relevant parts are included in this model.

In this study, multiple submodels are introduced for different purposes as it can be seen in Fig.6. Submodeling is a finite element technique which enables to zoom into a region of interest, to refine the mesh and to get more accurate results.

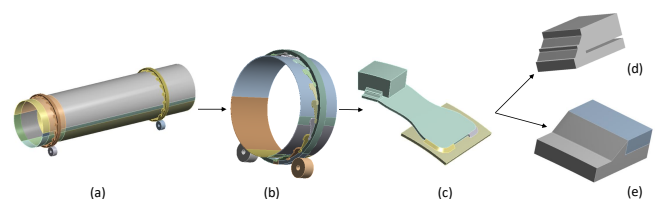


Fig. 6 Submodeling process

Firstly, the full model of the rotary kiln (a) is solved with a coarse mesh. Then, a submodel (b) is considered to compare strains with the strain gauge measurements, to locate the critical position of the spokes and to extract results for fatigue analysis. Once the critical position is determined, a new submodel (c) is made to be used to find a better design of spoke using shape optimization. Finally, two submodels (d) and (e) are placed on each weld of the spoke considered in order to apply the notch stress method for fatigue assessment of welded joints.

3.2 Mesh and Boundary Conditions

Once the modeling part is done, the structure should be discretized that is to say divided into a series of simple elements defined by n nodes [5]. For static analysis, higher order 3D SOLID186 elements are used.

Defining the most suitable boundary conditions is crucial in FEA, even more for thermo-mechanical analysis where both thermal and structural boundary conditions have to be determined. Rollers are considered as cylindrical fixed supports. Their contact with the ring is defined as *No Separation* contact due to its ability to allow some small sliding. It is assumed that the displacements are small compared to the length of the rotary kiln.

The thermal load should be applied according to the data mentioned in section 2.2. This means that the same temperature distribution and emissivity captured by the IR camera are used in the model. Moreover, heat transfer coefficient is considered for the spokes due to the convection (see Fig.7).

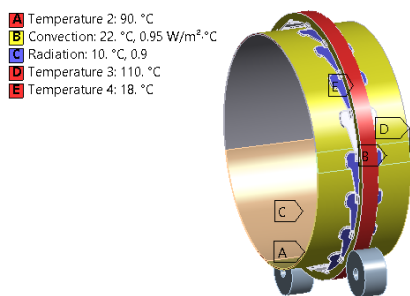


Fig. 7 Boundary conditions for the thermal analysis performed on submodel (b)

By importing the nodal temperatures from the steady-state thermal analysis into the static structural scheme, thermal stresses are computed. By adding static loads as pressure acting on the drum shell, boundary conditions are completed.

3.3 Numerical Results

After solving the FEA submodel Fig.6 (b), stress results can be extracted and evaluated. As seen in Fig.8, the maximum principal stress (σ_1) is noticed highest on the spoke at the identified reference point. The maximum principal stress remains highest at the reference point throughout one revolution of the kiln.

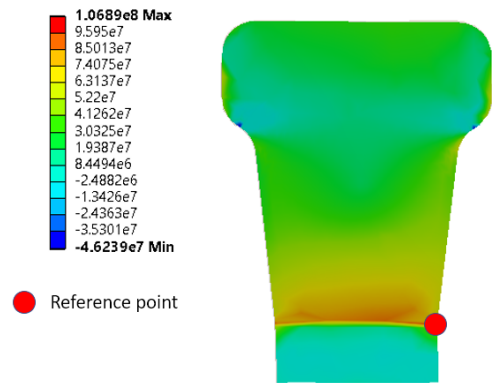


Fig. 8 Maximum principal stresses at the critical position of the spoke

Recalling Fig.2, it can be said that the FEA model is validated by the existence of the crack at the same location as in the reference point. In order to evaluate this effect of this high stress on the lifetime, a fatigue analysis is essential to be carried out. To do so, a cyclic load is extracted using the submodel presented in Fig.9 to obtain the maximum principal stresses from the same reference point for eighteen spokes. This illustrates the stress variation through one revolution. Noted that small additional rotations are done in order to have a satisfactory overview of the stress range. Results are represented in Tab.II with the same numeration as in Fig.9.

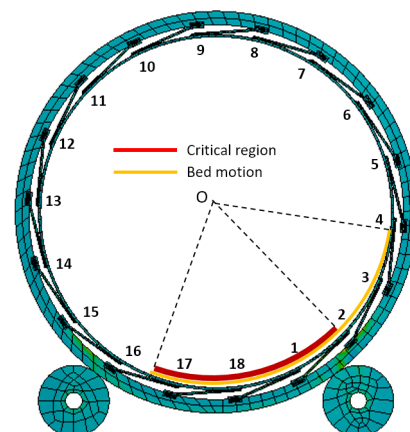


Fig. 9 Submodel with critical region where σ_1 is maximum

Also, it can be seen in Tab.II that a critical region exists between the two rollers as predicted in section 2.1.

Spoke	Max. Principal Stress	Spoke	Max. Principal Stress
1	103.21 MPa	10	49.76MPa
2	10.49 MPa	11	37.38 MPa
3	4.62 MPa	12	33.93 MPa
4	11.19 MPa	13	35.43 MPa
5	41.06 MPa	14	56.57 MPa
6	42.09 MPa	15	39.21 MPa
7	33.9 MPa	16	5.31 MPa
8	15.97 MPa	17	87.81 MPa
9	52.81 MPa	18	97.01 MPa

Tab. II Maximum principal stresses obtained from the spokes (see Fig.9) at the reference point (see Fig.8)

4. Wireless Strain Gauge Experiment

To verify if the assumptions taken for the numerical model built in FEA are correct, strain gauge experiment on an operating rotary kiln in an asphalt plant is done. To perform such an experiment, a wireless strain gauge setup is used which consists of different components including a strain gauge (input sensor), a wireless node (transmitter), a gateway (receiver) and a specific software to save the data [6].

In the experiment conducted for this article, one single strain gauge is attached on a spoke on the cold side of the rotary kiln. After the setup and the calibration done, the rotary kiln starts operating. Then data is recorded once the rotary kiln has reached a steady-state condition. It means that the raw material is introduced within the kiln rotating with a constant speed of 8 rpm and the temperature field is steady along its length.

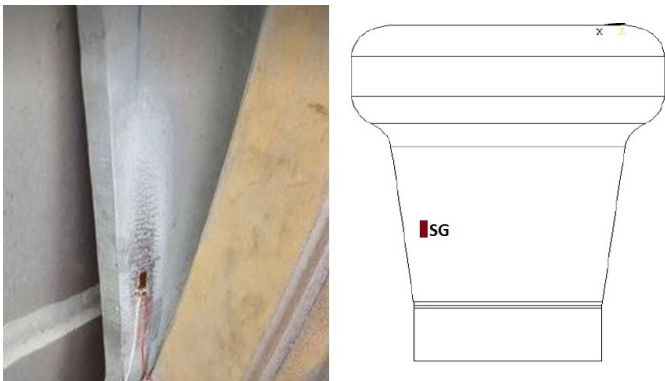


Fig. 10 Strain gauge location on rotary kiln and CAD model

The location where the strain gauge is attached during the experiment is as well considered in the numerical model (see Fig.10). Afterwards, normal strains are extracted from the eighteen FEA spokes. For one revolution of the rotary kiln, both strain results are

plotted in Fig.11. The shape of these two curves seems similar and cohesive.

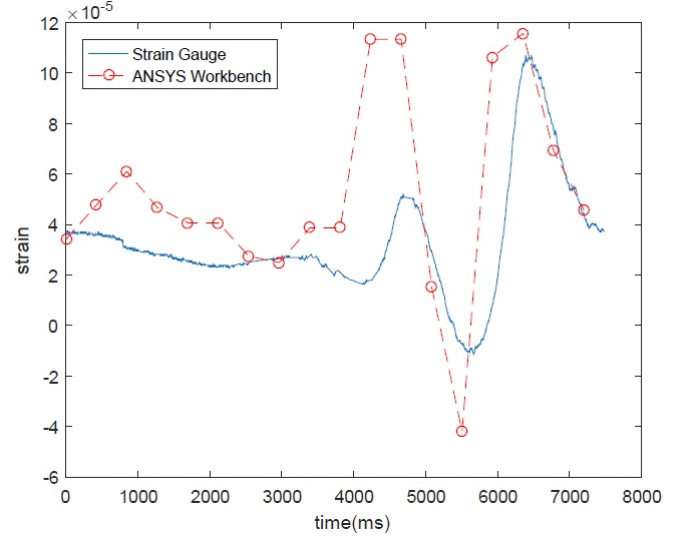


Fig. 11 Experimental and numerical results on eighteen spokes for one revolution of the rotary kiln

The maximum peak for the strain gauge is located in the area where the bed motion ends. The other maximum is situated between the two rollers. Also, two strain minima are observed when the spoke passes through the rollers.

For the strain gauge measurements, it can be explained that one peak is higher than the other by the fact that in reality the temperature field is not evenly distributed along the cross section. In fact, the bed motion which is unevenly distributed conducts heat implying some additional thermal load at its location.

It is worth mentioning that the values from the numerical model are shrunk by a factor of three in Fig.11. Two main explanations have been formulated about the overestimation of the FEA model compared to the strain gauge measurements:

- Either one software parameter called *Slope*, determined automatically after strain gauge calibration, is not reliable and gives lower strain gauge results. To extract strains from the data collected by the software, Eq.5 must be used [7].

$$Output = Slope * Bits + Offset \quad (5)$$

Using a slope three times higher, the results for both strain gauge measurements and the numerical model would be comparable.

- Or the contacts assumed in FEA are too conservative.

5. Fatigue Analysis

The definition of fatigue is the process of progressive localized permanent structural change occurring in a material subjected to conditions that produce fluctuating stresses and strains at some points which may culminate in cracks or complete fracture after a sufficient number of fluctuations [8]. As mentioned before, fatigue plays a major role in the failure of both the spoke and the welds. It is therefore vital to introduce fatigue assessment approaches to evaluate the lifetime of the spoke and the welds based on the analysis conducted in section 3.

5.1 Fatigue of Welded Joints

There are different fatigue strength assessment approaches that can be used to evaluate the fatigue lifetime of welded joints. In this work, the notch stress approach is used for this evaluation process since it is found to be the most suitable. This is in regard to the size and complexity of the components of the rotary kiln, and it also fits best with the current FEA models. The approach is very flexible in the sense that both the toe and the root of all types of welded joints can be assessed using a single S-N curve [9].

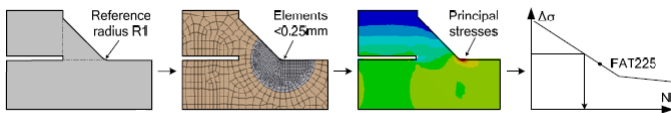


Fig. 12 Schematic principles of fatigue assessment using the notch stress approach [9]

The basic work flow of this approach is illustrated in Fig.12. The notch stress approach correlates the stress range in a fictitious rounding in the weld toe or root to the fatigue life using a single S-N curve. The notch stress is typically calculated using finite element models, which is also suggested from the IIW recommendations [10], with a reference radius of 1mm (the notch) to avoid the presence of stress singularities in sharp notches. A very fine mesh is needed so that the local stresses can converge. It is indicated by Fricke [11] that quadratic elements should be used with maximum element length of 0.25mm in the case of a 1mm notch radius. In this paper, the notch stresses are calculated using the largest numerical principal stress range and assessed against a S-N curve, commonly the fatigue class of FAT225 as indicated by Sonsino [12].

As mentioned before, a fine meshed region is needed towards the notch area to get accurate stresses. Therefore,

the submodeling technique is applied as seen in Fig.6. The principal stresses are then extracted accordingly as presented in Tab.III.

Position	σ_1	σ_2	σ_3
Ring	70 MPa	-55 MPa	1,35 MPa
Shell	18 MPa	-133 MPa	-12 MPa

Tab. III Principal Stresses on welds at ring and shell

Based on the values in Tab.III, the largest numerical principal stress range for both welds located on the ring and the shell, as seen in figure 6, are computed. The calculation procedure is formulated in Eq.6. It is worth mentioning that the stress range is conservatively calculated to obtain a maximum value. Note that σ_{ref} , which is the value of principal stress when the rotary kiln is not loaded, is set to 0.

$$\begin{aligned} \text{Ring: } \Delta\sigma_R &= \sigma_1 - \sigma_{ref} = 70\text{MPa} \\ \text{Shell: } \Delta\sigma_S &= \sigma_{ref} - \sigma_2 = 133\text{MPa} \end{aligned} \quad (6)$$

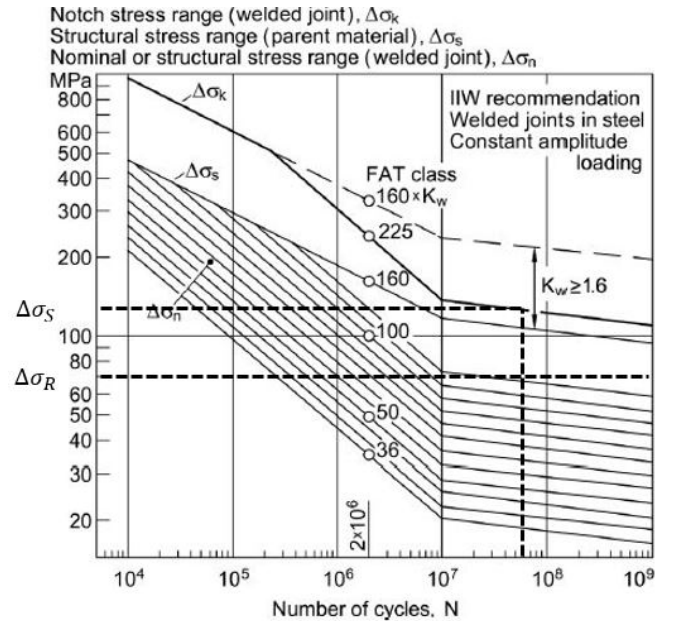


Fig. 13 S-N curve of fatigue class in terms of the notch stress (FAT225) [11]

According to the fatigue curve of FAT225 and the values obtained as seen in Fig.13, the weld on the ring has an infinite lifetime while the weld on the shell has an expected lifetime of $6 \cdot 10^7$ which is considered too large. This conclusion is expected since investigation shows that far away from the burner (i.e. cold side) only the spokes failed at the ring and not the welds. It is therefore reasonable to obtain such results for the fatigue lifetime of the welds.

5.2 Fatigue Analysis of Spoke

Components and structures are continuously subjected to quite diverse load histories. At one extreme, their histories may be rather simple and repetitive, also known as the *constant amplitude loading*. At the other extreme, they may be completely random, also referred to as *variable amplitude loading* in this case [8].

It is important to point out that the spokes studied are subjected to a load that varies during operation, that is to say a variable amplitude loading. In this case, a method is needed in order to deal with such situation since this variable amplitude spectrum is not suitable for direct use of S-N curve.

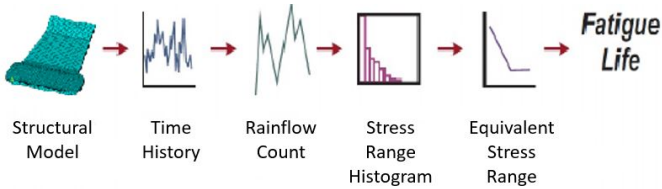


Fig. 14 Variable amplitude loading model

To estimate the fatigue life of the spoke, the schematic shown in Fig.14 is followed accordingly. The procedure starts by calculating the first principal stress, σ_1 , at a certain reference point from the FEA model as shown in Fig.8. At this location, the stresses are at a maximum throughout the entire operation. This reference point is the same location where actual cracks propagate and failure occurs at the spoke, as seen in Fig.2. The extracted principal stresses are plotted in a time history graph, as illustrated in Fig.15, where rainflow counting method can afterwards be applied.

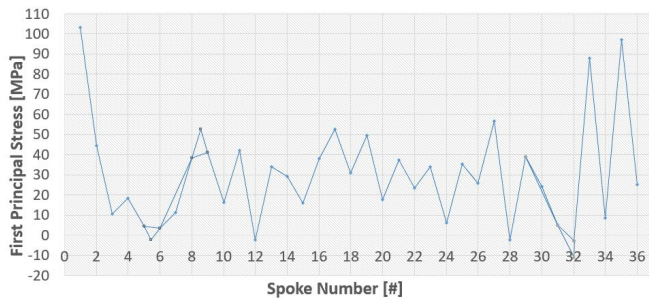


Fig. 15 Load history diagram

Rainflow counting method is considered as one of the best methods for cycle counting [8]. This method identifies all of the stress ranges as well as indicating all reversals. In the next step, the stress ranges $\Delta\sigma_i$ are grouped in suitable intervals. The total number of cycles

n_i in each interval corresponds to half the number of reversals. The results from this procedure are shown in Tab.IV.

$\Delta\sigma$ [MPa]	$2 \cdot n_i$	n_i	$\Delta\sigma_i$	$n_i(\Delta\sigma_i)^3$
0-15	6	3	7.5	1265.625(*)
15-35	7	3.5	25	54687.5(*)
35-55	5	2.5	45	227812.5(*)
55-75	4	2	65	549250(*)
75-95	2	1	85	614125
95-115	2	1	105	1157627
Σ	4	2	—	1771752

Tab. IV Procedure of rainflow counting

From Tab.IV, the concept of an equivalent stress range to correlate data from variable amplitude cyclic load tests with data from constant amplitude tests can now be implemented. The concept states that, for the same number of cycles, the equivalent (constant amplitude) stress range will cause the same fatigue damage as the sequence of variable amplitude stress ranges it replaces [13]. The equivalent stress range can be expressed as Eq.7.

$$\Delta\sigma_{eq} = \left(\frac{\sum (n_i (\Delta\sigma_i)^m)}{\sum n_i} \right)^{\frac{1}{m}} \quad (7)$$

Substituting the values in Tab.IV into Eq.7, the equivalent stress is therefore equal to $\Delta\sigma_{eq} = 96 \text{ MPa}$. It is now possible to read off the allowable equivalent number of cycle $n_{f,eq}$ as seen from Fig.16. The value approximately corresponds to $n_{f,eq} = 4 \cdot 10^6$. The S-N curve used is of detail category 125 from the Eurocode standards [14] as it fits the specifications and description of the spoke.

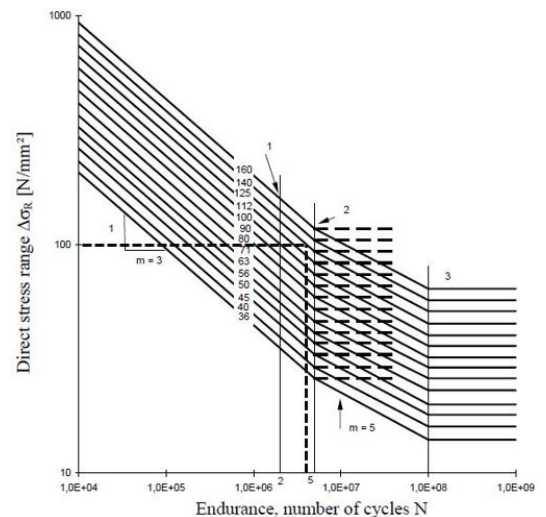


Fig. 16 Allowable equivalent number of cycles $n_{f,eq}$ [14]

The damage D caused by the equivalent stress range can be calculated using Eq.8. It is stated that no damage occurs if $D \leq 1$. Also, the lifetime of the spoke is evaluated using Eq.9 where $time$ corresponds to one revolution of the rotary kiln and is equal to 7.5 s. The total life is expected to be 4166h of operating time.

$$D = \frac{\sum n_i}{n_{f,eq}} \quad (8)$$

$$t_f = \frac{n_{f,eq}}{\sum n_i} \cdot time = 4166h \quad (9)$$

If it is assumed that the rotary kiln operates eight hours per day, failure is then expected to occur on the spoke after 520 days.

6. Optimization

The basic concept of optimization is to find a solution which can minimize the objective (cost) function subjected to several equality and inequality constraints. In order to increase life time of the spokes, the objective function is set to be the maximum principal stress. To find the optimum design, one approach with MATLAB and the other one with ANSYS Workbench are considered. Combining the results from two approaches, the new design of spoke is presented and evaluated in the end.

6.1 Optimization in MATLAB

The optimization is carried out by MATLAB build-in optimizer "fmincon" with gradient based algorithm sequential quadratic programming (SQP) [15]. A batch file of ANSYS APDL is created containing the information of model geometry, design variables, mesh, boundary conditions and data outputs. This batch file is used as a function to run evaluations and provides the necessary information for further optimization. The model geometry, containing only one spoke without any welding, is built using bottom-up modeling. Hence, it is possible to analyze the new model at each iteration when one point (i.e. design variable) is moved during optimization. It should be emphasized that the boundary conditions are taken from the result of ANSYS Workbench submodeling. Due to the lack of contact stress information in Workbench, the stresses are lower in APDL. However, the contours of stress in both models are very similar. In conclusion, the optimization result of this model is served as a first guess which should be evaluated carefully.

Additionally, multi-objective function is applied in the interest of obtaining a better result. The procedure is described as follows (a) sort the maximum principal stress values in a descending order (b) select the first 500 values to be the objective functions f_k , k is 1 to 500 (c) treat the functions with Kreisselmeier-Steinhauser (KS) function (Eq.10) and set it to be the final objective function. Note that ρ is taken as 4 in this case. f^{max} is the largest value among the objective functions and n is the number of objective functions.

$$f_{KS} = f^{max} + \frac{1}{\rho} \log \left(\sum_{k=1}^n e^{\rho(f_k - f^{max})} \right) \quad (10)$$

Fig.17 shows the design variables (DV) set up and the comparison of original and optimized shape. There are eight points set on the boundary of the model with different constraints. Note that the bound indicates the design variables can only move in horizontal direction. The maximum principal stress on the optimized spoke is reduced by 15% compare to the value of original spoke.

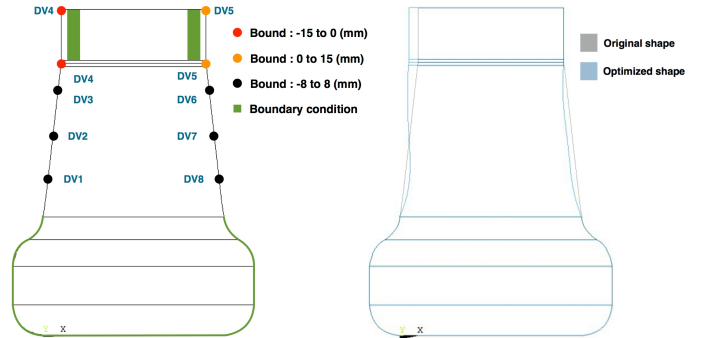


Fig. 17 Design variables set up and result in MATLAB

6.2 Optimization in ANSYS

Given the insufficiency of the MATLAB script to optimize main dimensions of the spoke, an other approach using ANSYS Workbench is used. The built-in optimizer ANSYS DesignXplorer enables to solve optimization problems with different algorithms including the so called Multi-Objective Genetic Algorithm (MOGA)[16]. Genetic Algorithm (GA) is a meta-heuristic relying on bio-inspired operators such as mutation, crossover and natural selection to generate a new population [17]. This optimization method is therefore used to avoid the possibility of trapping in a local minimum.

There are two objective functions considered in the problem. The first one (high priority objective function) concerns maximum principal stress on a path of the

spoke, where the critical point is located. The second one concerns maximum principal stress on the surface of the spoke in order to monitor any shift of the critical point. Five parameters of the spoke are defined in this optimization problem as shown in Fig.18.

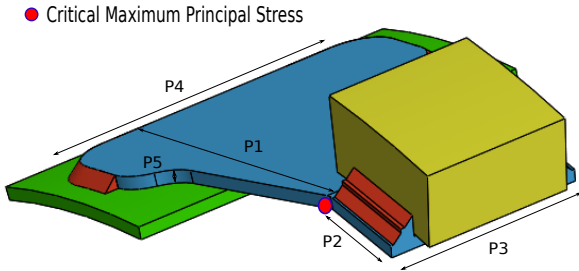


Fig. 18 Optimization parameters defined on the spoke

After eight numbers of MOGA iterations, the best candidate point is returned by DesignXplorer. It shows that the maximum principal stress of the critical point has reduced from 121 MPa to 86.8 MPa, which implies a 28% reduction. The bounds and optimized values of parameters are given in Tab.V. It can be noticed that after optimization all these parameters are close to the lower bounds defined.

Parameters	Lower bound	Upper bound	Optimized value
P1 (mm)	420	455	421,7
P2 (mm)	85	105	86,3
P3 (mm)	240	280	247,9
P4 (mm)	350	420	353,3
P5 (mm)	12	25	12,4

Tab. V Bounds and optimized values of input parameters

6.3 Results evaluation

Combining both approaches in MATLAB and ANSYS, a new design of the spoke and maximum principal stress distribution are presented in Fig.19. After modeling the ring with the newly optimized spokes in the FEA model, the fatigue lifetime is calculated for these new spokes using the same procedure as described in section 5. The new effective stress range is $\Delta\sigma_{eq} = 85MPa$, which is reduced by 11.5%. Furthermore, the lifetime is expected to be approximately 868 days, which results in an increase by 67%.

By changing the shape of the spoke, the stress is redistributed and moved away from the previously concentrated area. Additionally, the reduction of length overcomes the large shear force introduced by the expansion of the drum. Note that both optimization in

MATLAB and ANSYS are performed on one spoke only (i.e. one critical position during operation). This indicates that the new design is not necessarily better for all other positions. Hopefully this problem has not been encountered during the redesign process. However, for a more comprehensive optimization approach, the maximum principal stresses on all eighteen spokes in the model should be considered at the same time using multi-objective functions.

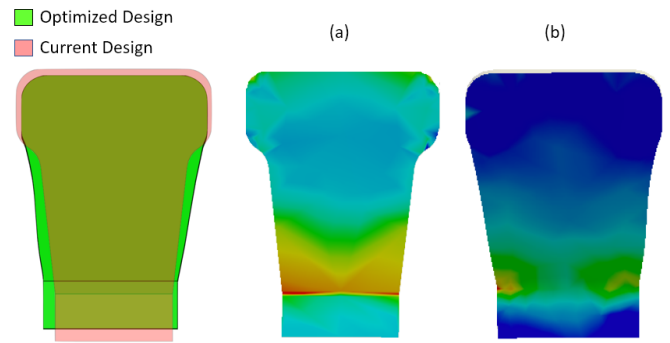


Fig. 19 Results of (a) original spoke (b) optimized spoke

7. Conclusion

Thermal and mechanical loads acting on the rotary kiln highly reduce the fatigue life of the spokes, causing cracks and implying costly repairing operations. An analysis and redesign of the spokes located on the cold side have been presented in this paper to overcome this issue. After solving the numerical model of the structure and performing the fatigue analysis, a realistic lifetime for current spokes has been found. In fact, while carrying out the strain gauge measurements, it has been noticed cracks at the critical FEA locations on the cold side of a three-year old operating kiln. By keeping the same manufacturing process, the newly optimized spoke increases the current spoke's lifetime by 67%. However, the redesign presented here is probably not the best possible one. Indeed, performing both shape optimization and optimization on main dimensions using ANSYS DesignXplorer would have most likely provided a better designed spoke. In addition, attention should be given to the other spokes as their stresses may possibly go up. Different parameters not directly studied could play a role to reduce the stress on the spokes such as the angle of rollers or the orientation of spokes with respect to the rotation of the kiln. If the study would have been focused on the so called hot side, stresses would have been much more significant, especially around the welded joints, and a more drastic redesign should have been considered.

Acknowledgement

The authors of this work gratefully acknowledge Sintex for sponsoring the 5th MechMan symposium.

References

- [1] A. A. Boateng, Rotary Kiln. Elsevier, 2008.
- [2] A. Z. et al, “Analytical and numerical stress analysis of the rotary kiln ring,”
- [3] Y. A. Cengel, Heat Transfer. Mcgraw-Hill, 2nd ed., 2002.
- [4] “Keysight technologies how to measure the unknown thermal emissivity of objects/materials using the u5855a trueir thermal imager,” 2015.
- [5] Cook et al, Concepts and applications of finite element analysis. Wiley, 3rd ed., 2002.
- [6] “Lord user manual, v-link-lxrs wireless 7 channel analog input sensor node1,” 2015.
- [7] “User guide version 8500-0017 rev 001 little, wsda-base-101 analog output base station1,” 2011.
- [8] Stephens1, Metal Fatigue in Engineering. Mcgraw-Hill, 2nd ed., 2000.
- [9] O. s. H. M. R. A. J. G. Pedersen, Mikkel Melters; Mouritsen, “Experience with the notch stress approach for fatigue assessment of welded joints,” 2010.
- [10] A. Hobbacher, Recommendations for Fatigue Design of Welded Joints and Components. Springer, 2nd ed., 2014.
- [11] W. Fricke, “Iiw recommendations for the fatigue assessment of welded structures by notch1,” 2010.
- [12] C.M.Sonsino, “A consideration of allowable equivalent stresses for fatigue design of welded joints according to the notch stress concept with the reference radii $r_{ref} = 1.00$ and 0.05 mm,” 2009.
- [13] J.M.Bloom, Probabilistic Fracture Mechanics and Fatigue Methods. STP 798, 1st ed., 1983.
- [14] “Eurocode 3,” 2007.
- [15] J. S. Arora, Introduction to Optimum Design. 4th ed., 2017.
- [16] “Design xploration user guide,” 2015.
- [17] A. S. A. Konak, D.W. Coit, “Multi-objective optimiation using genetic algorithms: a tutorial,” Elsevier, pp. 993–995, 2005.